



Article

Improving SWAT Model Calibration Using Soil MERGE (SMERGE)

Kenneth J. Tobin * and Marvin E. Bennett

Center for Earth and Environmental Studies, Texas A&M International University, Laredo, TX 78045, USA; mbennett@tamiu.edu

* Correspondence: ktobin@tamiu.edu; Tel.: +1-956-326-2417

Received: 13 May 2020; Accepted: 14 July 2020; Published: 18 July 2020



Abstract: This study examined eight Great Plains moderate-sized (832 to 4892 km²) watersheds. The Soil and Water Assessment Tool (SWAT) autocalibration routine SUFI-2 was executed using twenty-three model parameters, from 1995 to 2015 in each basin, to identify highly sensitive parameters (HSP). The model was then run on a year-by-year basis, generating optimal parameter values for each year (1995 to 2015). HSP were correlated against annual precipitation (Parameter-elevation Regressions on Independent Slopes Model—PRISM) and root zone soil moisture (Soil MERGE—SMERGE 2.0) anomaly data. HSP with robust correlation (r > 0.5) were used to calibrate the model on an annual basis (2016 to 2018). Results were compared against a baseline simulation, in which optimal parameters were obtained by running the model for the entire period (1992 to 2015). This approach improved performance for annual simulations generated from 2016 to 2018. SMERGE 2.0 produced more robust results compared with the PRISM product. The main virtue of this approach is that it constrains parameter space, minimizesing equifinality and promotesing modeling based on more physically realistic parameter values.

Keywords: SMERGE 2.0; PRISM; root zone soil moisture; SWAT; US Great Plains; mass balance

1. Introduction

The Soil and Water Assessment Tool (SWAT) is a physically based model with demonstrated global applications and has been validated at the watershed scale through the publication of thousands of referred papers (see [1]). The SWAT model is moderate in terms of complexity, i.e., it is a semi-distributed model where the watershed is divided into subbasins, in which water balance is calculated on a daily basis. Many SWAT modeling studies have focused on matching simulated and observed streamflow at the basin's outlet. Calibration based on multiple gauges within a basin has been demonstrated to more realistically capture surface flow throughout an entire watershed (e.g., [2,3]). However, this approach, while an improvement, can fail to provide a realistic depiction of landscape conditions that strongly influence runoff production. During recent years, hydrologists have begun to leverage remote sensing observations to improve model calibration and achieve a more accurate picture of processes at a watershed scale. Examples of such studies that utilized the SWAT model span diverse aspects of the hydrologic cycle and include quantifying total terrestrial water [4,5], soil moisture [6–8], evapotranspiration [9–11], and groundwater recharge [12,13].

Since SWAT was designed as a tool to first and foremost simulate runoff, issues can arise when simulating other fluxes and state variables, such as soil moisture or evapotranspiration. New approaches have been developed to facilitate the incorporation of remotely sensed data to support watershed scale studies [14]. Of particular promise are data assimilation (DA) techniques adopted from the atmospheric science community, which have been increasingly applied to watershed hydrology studies [15–17]. However, the improvements that can be potentially conferred by DA have limitations. DA has difficulty

Water 2020, 12, 2039 2 of 21

in improving streamflow performance under high flow conditions [15,16] because runoff production is largely decoupled from the control of soil moisture under these circumstances. In addition, SWAT has some structural issues related to how soil moisture is accounted for that limits the benefits of DA of root zone soil moisture (RZSM) in this model. For example, the authors in reference [17] used DA to incorporate RZSM into SWAT and achieved worse results than open loop simulations. This is because the physics of the SWAT model without modification are not sufficiently complicated to account for vertical coupling between different soil layers. Despite these issues, soil moisture remains an important control on surface runoff production. One of the most important parameters within SWAT is the Curve Number (CN2), which is initialized based on the moisture content within soils. Therefore, finding a way of leveraging soil moisture to support more realistic modeling of streamflow remains important.

Another approach that provides a more holistic prospective is a mass balance accounting of the overall water budget. This method has yielded meaningful insights particularly at the regional and watershed scales (e.g., [18–20]). In reference [21], it is indicated that inter-seasonal and inter-annual variations in surface water storage volumes, as well as their impact on precipitation (P), evapotranspiration (ET), surface water storage (S), and runoff (Q), are not well understood. There remains a fundamental lack of knowledge, both in terms of spatial and temporal scales, regarding the hydrologic processes that influence each of the terms of the basic hydrologic equation. Incorporation of multiple observations (both in situ and remotely sensing) into model calibration can force modeling to be based on more realistic parameter selection. Therefore, the objective of this study is to demonstrate whether diverse remote sensing observations can improve simulated SWAT streamflow in eight Great Plains watersheds.

2. Watersheds Examined

Eight, moderate-sized (832 to 4892 square km) watersheds were examined (Table 1; Figure 1). Basins generally have a dendritic drainage pattern with a rounded shape, except for Chickaskia (CH) and Ninnescah (NI), which are elongated. Bird Creek (BC), CH, Little Arkansas (LA), and Little Nemaha (LN) flow in general toward the southeast. Black Vermillion (BV) drainage is oriented southwest and Walnut (WN) toward the south. Mill Creek (MC) and NI flow toward the east. The SWAT model is subdivided into subbasins as computational units. To enhance inter-comparability of the results, the number of subbasins was set as consistently as possible. The eight basins had subdued topography typical of the Great Plains region. Overall relief varied between 130 to 313 m in the examined watersheds (Table 1). In terms of soils, most watersheds were dominated by some variants of loam within the top layer that roughly correspond with the upper root zone. The only exception was NI, where loamy sand was the most abundant texture. Land use/land cover in five watersheds was dominated by agricultural activity (BV, CH, LA, LN, NI). BC, MC, and WN also had significant rangeland and grasses.

Elevation **Dominant Soil Dominant Land Basin** Subbasins Size (sq. km.) (m) Texture Cover Bird Creek (BC) 31 177 to 403 Rangeland/Grass 2360 Loam Black Vermillion (BV) 1071 31 338 to 468 Clay Loam Agricultural 4892 33 295 to 608 Chickaskia (CH) Silt Loam Agricultural Little Arkansas (LA) 3402 33 409 to 544 Silt Loam Agricultural Little Nemaha (LN) 31 2061 274 to 444 Clay Agricultural Mill Creek (MC) 29 Silt Clay Loam 832 291 to 488 Rangeland/Grass Ninnescah (NI) 2049 35 446 to 637 Loamy Sand Agricultural Walnut (WN) 4855 33 330 to 512 Silt Loam Rangeland/Grass

Table 1. Watershed characteristics.

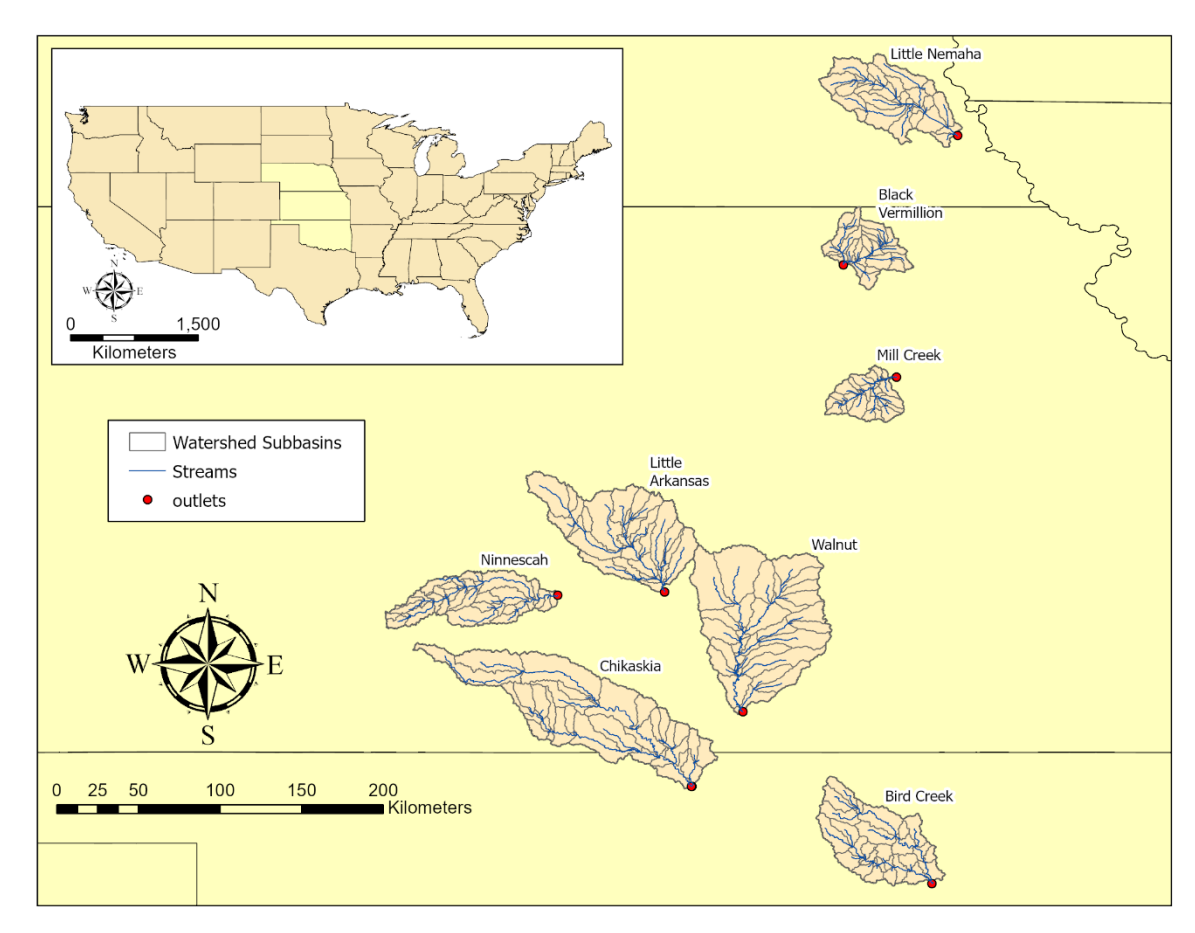


Figure 1. Locality map illustrating the position of the eight examined watersheds. **Figure 1.** Locality map illustrating the position of the eight examined watersheds.

3. Datasets Used

3. Datasets Used

- 3.1. SWAT Model Input
- $^{3.1.}$ SWAT Model Input incorporates landscape information about elevation, soils, and land use/land covert Helenation in attenue continued of tomathap National Maps Down lead acronic softing anticellations estates Condective Surves a Talor of this reach the sport of war and many loaded time and are found to without spatial seads tien log Lat Gerood Tiles op its is be Digisal General weit Mop alche United States on 8TATAGO2 (United States (US) Dop of more second indress Machington, Clack's Side valoped by the Ustines GOSPATTSCO2011 SWEET Staves CESPEDE dar Thierproductival under what ded through the Natural Resources the marketing Servicative son the Parta Casterion in 17 Dispose the partie down as a delitions and inherent N250/00 Reportation of the Alari danger with a decorated at the continuous for the particular data and the continuous for the c Action consisted the four of 250 has Newtonian Control Francisco Characteristic Patricular and The Patricular Control Francisco Characteristic Patricular Characteri Nevel apellaby the Multi-Resolutions bend Characteristica Causertium atoms entreined in a fall of the content o Currentawill has special as solution alogo arby the Multi-Resolution Land Characteristics Consortium. It was disparrentera (Glogith data (ataly)) presipitations and tompeson une) were obtained from the PRISM Climate Groupted Otogoal State University: That product the part I know patiel obsolution on which Rabor ChinantiGeotal Michael StastatiCONNES); iTo Thipport duer ution of the SNAAT resolutionity PRISM adata the all-AWA-T-authorist Sures a Codetes vilog copolistation to have those who to to continue the continue to t tollaniswach subbasins was labiting edwushly as in avidatiswas pased graphitatios evitor obtains Mograll eighthasiachysbhadiavaragingon, annual basin-wide averages for precipitation were obtained for all eight basins by simple averaging. 3.2. Other Soft Data
- 3.2. Of the RESMP, the SMERGE 2.0 product (US National Aeronautics and Space Administration, NASA, Washington, LISA) was relected [32] This product provided particularly robust results NASA, Washington, DC, USA) was selected [22]. This product provided particularly robust results

Water 2020, 12, 2039 4 of 21

Plains region and reflects a product that blends equally remote sensing and land surface model datasets. SMERGE 2.0 is available at a daily time step and has a 0.125-degree spatial resolution. Like with PRISM precipitation data, SMERGE was averaged for each of the eight basins on an annual basis (1992 to 2018). Unlike PRISM data anomalies, not raw volumetric data were used for RZSM.

Three ET products were applied to this study (Moderate Resolution Imagining Spectrometer, MODIS16A2v5, US NASA Earth Observing System Data and Information System (EOSDIS) Land Processes Distributed Active Archive Center (DAAC), [23]; Simplified Surface Energy Balance, SSEBopv4, US Geologic Survey, Center for Integrated Data Analytics, Middleton, Wisconsin [24]; Global Land Evaporation: the Amsterdam Model, GLEAMv3.3a, Vrije Universiteit Amsterdam, The Netherlands [25]). The MODIS product was obtained in a monthly HDF file with a 1 km resolution. This dataset was extracted into a raster layer and zonal statistics tools were utilized to obtain the average of the pixels intersecting with the watershed outline. The same method was applied to SSEBop, which was obtained in a GeoTiff raster format with a 0.009-degree spatial resolution in monthly files. GLEAM was available in netCDF files in a grid of 0.25×0.25 degrees with a monthly temporal resolution. The values of the grids with centroids within the watershed were extracted and summed to obtain the average. Values were summed to calculate an annual estimate of ET (2016–2018) for the eight examined watersheds.

Total terrestrial water was estimated from the NASA Gravity Recovery and Climate Experiment (GRACE) using the GRCTellus JPL-Mascons dataset [26,27]. This product combined monthly gravity solutions from GRACE and GRACE-FO, as determined from the JPL RL06Mv2 mascon solution with the coastline resolution improvement filter. The GRACE product was available in a monthly netCDf file (missing values exist) at a 0.5-degree spatial resolution. The average of intersecting GRACE grids with the watershed was summed to obtain an annual estimate (2015–2018) of total terrestrial water change.

Finally, to constrain an interception-related SWAT parameter, the MOD15A2H Terra version 006 combined Leaf Area Index (LAI) and Fraction of Photosynthetically Active Radiation (US NASA EOSDIS Land Processes DAAC, Sioux Falls, ND, USA) was used [28]. This product had a 500 m spatial resolution and was an eight-day composite dataset based on the best available from acquisitions from each period. Values were aggregated to obtain a basin-wide estimate of LAI.

4. Methodology

4.1. SWAT Model Setup

In SWAT, the automatic watershed delineation tool was used to define the stream network and number of subbasins within a watershed. Subbasin number was based on the area of the watershed present upstream of the beginning point for each tributary channel. Within each subbasin, water balance calculations were based on the aerially weighted proportions of unique combinations of soil and land use, referred to as hydrologic response units (HRU). Each HRU had a unique Curve Number (CN), adjusted for antecedent moisture conditions, which was used to determine infiltration and surface runoff within each subbasin. Another component of the SWAT model that enhanced its ability to calculate the water balance within each subbasin was the calculation of daily potential evapotranspiration values using the Priestley–Taylor method [29]. SWAT does not consider the spatial location of HRUs within each subbasin, and consequently, this is why SWAT is not considered a fully distributed model. Excessive runoff generated within each subbasin was conceptually routed as overland flow. Once overland flow water intersected a stream reach or channel, water was routed downstream using the variable storage method [30].

Water 2020, 12, 2039 5 of 21

To facilitate autocalibration of the SWAT model, the stand-alone SUFI-2 autocalibration [31] routine was utilized. Of the autocalibration programs available for the SWAT model, SUFI-2 converges on an optimal solution with a relatively small number of executed simulations (500 to 1000 model runs; [32,33]) and was ran at a daily time step. In addition, SUFI-2 provided an estimate of parameter sensitivity. Note that HRU parameter values were averaged at the subbasin level. Only highly sensitive parameters (HSP; *p*-value < 0.02) were varied after the first two global simulations executed, which are described below.

To evaluate model performance, standard objective measures were used, including the mass balance error (MBE) and Nash–Sutcliffe efficiency coefficients (NS). To collapse these metrics into one measure, all model results were evaluated based on the Relative Performance Scale [34]. This combined metric was based on the criterion of reference [35] (see Table 2). To calculate the RPS, both the MBE and NS were translated into a single RPS metric. For example, if a simulation has a NS = 0.75 and MBE of 15%, these values constituted provisional RPS values of 3.00 and 2.00, respectively. To be conservative, the lower provisional RPS value was always selected so that in this example, the final RPS value assigned was 2.00. The best model run for each simulation type was evaluated with a single RPS score to facilitate inter-comparison of results.

Description	Nash Sutcliffe (NS)	Mass Balance Error	Relative Performance Scale (RPS)
Perfect	1.00	0%	4.00
Very Good	0.75	10%	3.00
Good	0.65	15%	2.00
Satisfactory	0.50	25%	1.00
Unacceptable	< 0.50	>25%	<1.00

Table 2. The Relative Performance Scale (RPS).

4.2. Simulation Series

Three series of model runs were executed in this study and include: (1) global simulations (1995 to 2015); (2) individual year-by-year models runs for each year between (1995 to 2015); (3) final calibration year-by-year simulations (2016 to 2018). For all series, a three- to four-year warm up period was executed to initialize SWAT.

4.2.1. Global Simulation Series

For global simulations, one RPS value was calculated for the entire simulation period (1995 to 2015) in each watershed; shorter for MC (2005 to 2015). This simulation series consisted of two model runs. The initial simulation was referred to as Base_Q. In this model run, there were no constraints on parameters values, except for the outer bounds established by reference [29]. Parameter value ranges for the Base_Q are presented in Table 3.

The next type of global simulation consisted of iterative model runs, which constrained parameters to improve objective metrics and was referred to as IT_Q. Model parameters were limited in two ways: (a) using *a priori* data to set CANMX and ALPHA_BF and (b) examining Dotty plots (Figure 2) to identify limits for optimal performance for variable HSP. The CANMX parameter was set by using MODIS_LAI product and the following equation [36].

$$S_{\text{Max}} = f \log (1 + \text{LAI}) \tag{1}$$

where S_{Max} was the maximum water storage within the canopy, f was a specific factor dependent upon vegetation type, and LAI was determined from MODIS_LAI product (MOD15A2). ALPHA_BF was determined using the baseflow program from reference [37] and was set within a factor of two of the calculated value. Parameter sensitivity was examined and HSP were identified (Table 4). These parameters can be divided into two groups (variable and non-variable). Examination of Dotty Plots

Water 2020, 12, 2039 6 of 21

can further constrain variable, HSP values. While some of the parameters lack an optimal range of values (Figure 2a), others do not (Figure 2b). An iterative approach was used in adjusting parameters with optimal values to yield better performance. HSP specifically, in all basins, the tightening of the range of CH_K2 improved results. Additional iterations in BC and WN focused on CH_N2; in NI, with CN2; in WN, on OV_N. The tightening of variable HSP values had a beneficial impact on the final IT_Q model executed. From this simulation, the values of non-sensitive (p > 0.02) and non-variable HSP are set from the optimum parameter values calculated (Table 5). Only variable, HSP (Table 6) were left unconstrained in subsequent modeling series.

4.2.2. Individual Year-By-Year Series

Individual year-by-year model runs between 1995 to 2015 were executed. In this modeling series, objective results were obtained for each year (n = 21). All variable, HSP were correlated with annual SMERGE 2.0 RZSM anomalies and raw PRISM precipitation. Note that years with unacceptable RPS values were omitted from this analysis. Correlation values based on this modeling series weare presented in Table 7. The range and average for variable, HSP are shown in Table 8. Only parameters with a correlation (r) that exceeds 0.5 were considered in the third modeling series described next.

Table 3. Base_Q parameter ranges for all basins.

Parameter	Name	Low	High
CN2	Initial SCS runoff curve number for moisture condition II	35	95
ALPHA_BF	Baseflow Alpha Factor	0	1
GW_DELAY	Groundwater delay time (days)	30	450
CH_N2	Manning's "n" value for the main channel	0	0.3
CH_K2	Effective hydraulic conductivity in main channel alluvium (mm/h)	0	500
CH_N1	Manning's "n" value for the tributary channels	0	0.3
CH_K1	Effective hydraulic conductivity in tributary channel alluvium (mm/h)	0	300
OV_N	Manning's "n" value for overland flow	0.01	0.6
SURLAG	Surface runoff lag coefficient	1	34
GWQMN	Threshold depth of water in the shallow aquifer required for return flow to occur (mm H_2O)	0	5000
SOL_AWC	Available water capacity of the soil layer (mm H_2O/mm soil)	-0.2	0.4
ESCO	Soil evaporation compensation factor	0	1
GW_REVAP	Groundwater "revap" coefficient	0.02	0.2
REVAPMN	Threshold depth of water in the shallow aquifer for "revap" or percolation to the deep aquifer to occur (mm H ₂ O)	0	500
CANMX	Maximum canopy storage (mm H ₂ O)	0	100
EPCO	Plant uptake compensation factor	0	1
SFTMP	Snowfall temperature (°C)	-5	5
SMTMP	Snow melt base temperature (°C)	-5	5
SMFMX	Melt factor for snow on June 21 (mm H ₂ O/°C-day)	0	10
SMFMN	Melt factor for snow on Dec 21 (mm H ₂ O/°C-day)	0	10
TIMP	Snow pack temperature lag factor	0.01	1
SOL_K	Saturated hydraulic conductivity (mm/h)	-0.8	0.8
SOL_BD	Moist bulk density (g/cm ³)	-0.5	0.6

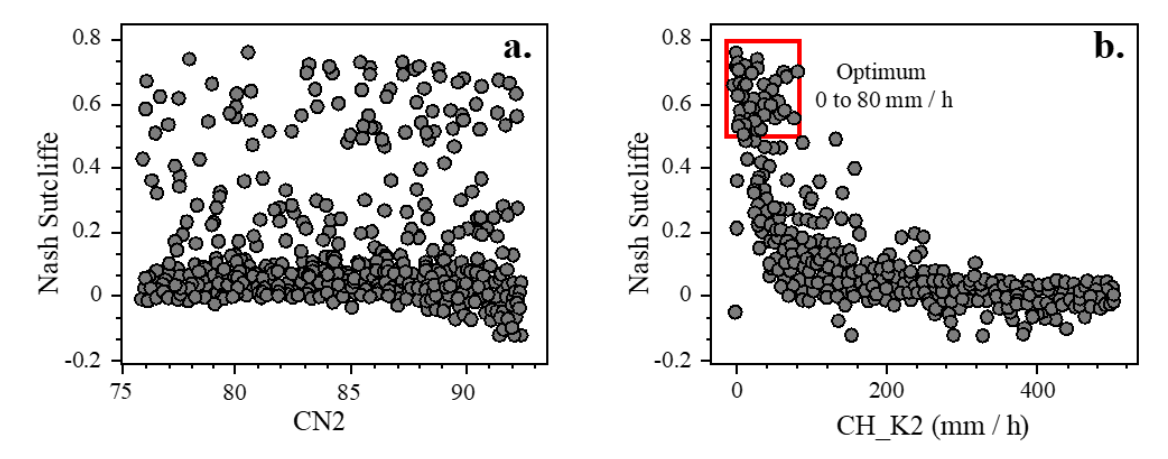


Figure 2. Dotty plots for BV basin. (a) NS versus CN2 and (b) NS versus CH_K2 parameter value with Figure 3. Dotty protest for BV basin. (a) NS versus CN2 and (b) NS versus CH_K2 parameter value with zone of optimum performance indicated.

Table 4. Highly	sensitive parameter	s (HSP) from	n IT (Simulation

	Basin Tab	le 4. Hig	hly sensit Variabl	ive paran e Parame	eters (HS ters	P) from I	T_Q simula - Non-Va	ition iriable I	Paramete	rs
Basin	ВС	Vana	blel Phra	nBetters:	N2, OV_N		on-MariBb			
ВС	BV CH ^{CN2}	, ALPH	N2 CH ALBENCI	7, Q <u>y</u> - Q	V=N, ESC	SC SC	CH_N2, A)L_BD, G\	WQMX	JF SOI , ESCO	AWC
BV		N2NEJH					V2, АЫДЫ	$A_{\Delta}B_{F_{F}}$	_br SMHTMHV	VC
CH					EGO GOL			<u> </u>		
LA	MSN2, C	H_N2, C	CHENEZ C			DD.	ALPHAN	BPYM	TEMITM!	P
LN	(N) (2, O)	/_N,sp	H_NZ, CI H2AWG		NTSOL SQL _C BD	BD	ALPHA_B	SMTM FMN N	IP J2. SOL.	AWC
MC -		_	CH_K2,	,	, 2000		H_N2, O			
NI	CN2, C	Hable 5	CHigh?v 9	SelfsitiveS	QL _{ar} BDer	s (HSP) fr	rom IT_&	TMPatio	on.	
WN_	C	N2, CH	_K2, OV	_N, ESC	0	ALPI	IA_BF, CI	<u>1_N2, 9</u>	SOL_AV	
_	Paramete					LA		1C	NI	WN
	ALPH Fal t						10 4Q 7simula 105 4	011∂n. ⊿3	0.033 166	0.0572 —189
Para	ameter _{N2}	BC	BV 0.	.25 5CH	LA	LN ().22 MC 0.	267 NI	100	0.065
ALP	HACH K2	3	9.0 180.112	0.0444	0.073	0,0427	3.20 0.012 0.049 0.012	0.033	0.057	2 2 12
	DELAY _{K1}			0091 0 99743.6	.300	$\frac{.084}{.38}105$	73.9 ⁴⁴³ 2	$\frac{254}{75}$ 166	$\frac{0.044}{123}$ 189	0.242 190
	H_ N 2V_N		0.255		20)	0.221	0.267 0.		0.065	
CI	H_StyRLAC					9.033.20		.02	20.5	3.92
CF	H GWQMN	0.184_{0}^{19}	$^{967}_{2000910}$	$\frac{342}{370}.300^{3}$	$\frac{3517}{350}.084_0^{-2}$	$\frac{2287}{0031}049$	$^{117}_{0.254}^{0.254}^{21}_{0.1}^{21}$	167 384.044_	4707 -0.125	$\frac{4552}{0.114}$
CI	H_K <u>ASCO</u>	11.0 0.	200 0. 043 2 97	239	83.8 0	.8673.9	275	123	0.186190	0.114
_	VGVV_REVA						0.159.582 0.		0.177	0.026
SU	REAGINA	$^{N}_{6.16}$	$\begin{array}{c} 653\\ 514 \end{array}$	66.2 _{16.3} .4050	337 _{9.03} 6	468 ₄ .84 .255	$\begin{array}{c} 4927.02 & 10.322 & 10.3$	9.2 368	138 ₃ .92 0.470	72.7 0.691
GW	/QMETCO	1967 0.	$86\frac{2}{3}342^{0}$.403 .433517 ₀	.73 6 287 0	.743 ¹ 17 ($0.322_{0.058}$ $167_{0.058}$	89 4 707	$0.470 \\ 0.254552$	0.891
SOL	_A \$\f CMP	0.268 - 2	2.38370-	4. 25 .352-	4.0200312	2.33 –	0.205384-0	.73%.125	-1.56114	10.905
	SCOMTMP				2.9 6 .865 0			.5 0 .186		-2.69
GW_{-}	REWAPMN	$0.118^{0.5}$	$^{093}_{.45}$ 0.056 $^{6}_{0}$	$0.46 \\ 0.077$	$\frac{0.965}{5.78} 0.068 \frac{7}{0}$	305.159	$\frac{1.40}{5.65}$ 0.191 $\frac{3}{4}$	$^{.38}_{.95}$.177	4.29.026	7.57
	APMMP	353 _{0.}	86 6 6.2 0.	.579337 0	.587468 0	.795492	0.73 \$ 9.2 0.	156138	0.6772.7	0.689
CA	NMQL_K					.036.322-				
<u>E</u>	PCOL_BD	0.863 ⁻⁰	$0.142_{-0.435}$ 0.	.339.736 ⁻¹	0.092 _{.743}	0.058	0.894^{-0}	.0 <u>86.254</u>	0.346	0.281
SF	TMP	-2.38	-4.25	-4.32	2.33	-0.245	-0.735	-1.56	0.905	5
SN	ИТМР	-0.845	1.24	2.96	0.975	0.765	4.51	4.98	-2.69)
SN	IFMX	0.095	6.46	0.965	7.46	1.40	3.38	9.49	9.70	
SM	IFMN	5.45	0.665	6.78	0.305	5.65	4.95	4.29	7.57	

Water **2020**, 12, 2039

Table 6.	IT C) SWAT	ranges for	parameters	that are	variable and HSP.
----------	------	--------	------------	------------	----------	-------------------

Parameter	BC	BV	СН	LA	LN	MC	NI	WN
CN2	60-84	76–92.4	72–88	68–84	68-84	70–88	45.9-80	76–90.3
ALPHA_BF	0.035-0.	139					0-0.3	
CH_N2	0.015-0.0	04	0-0.3	0-0.3		0 - 40	0 - 40	10-30
CH_K2		0-20	0 - 40	0 - 40	0.01-0.6		0.01 - 0.6	0.4 – 0.6
OV_N	0.01 - 0.6	0.01-0.6	0.01 - 0.6	0.01 - 0.6	-0.2 - 0.4			
ESCO		0 - 1.0	0 - 1.0		0 - 1.0	0 - 1.0		0 - 1.0
SOL_BD				-0.5-0.6	-0.5 - 0.6		-0.5 - 0.6	

Table 7. Parameter correlation (r) versus PRISM precipitation and SMERGE 2.0 root zone soil moisture anomalies based on individual year (1992 to 2015) runs.

	SMERGE 2.0								
Parameter	ВС	BV	СН	LA	LN	MC	NI	WN	
CN2	0.618	0.457	0.658	0.240	0.361	0.727	0.791	0.725	
ALPHA_BF	0.266								
CH_N2	0.114		-0.116	0.290			0.399	0.179	
CH_K2		0.191	0.324	0.345		0.129	-0.150	0.437	
OV_N	0.342	0.246	0.015	-0.437	-0.237		0.231		
SOL_AWC					0.048				
ESCO		-0.301			-0.251	-0.707			
SOL_BD				-0.450	-0.075		0.041		
			PR	ISM					
Parameter	BC	BV	СН	LA	LN	MC	NI	WN	
CN2	0.462	0.515	0.499	0.293	0.347	0.662	0.539	0.440	
ALPHA_BF	0.297								
CH_N2	0.031		-0.121	-0.052			0.329	0.321	
CH_K2		0.512	0.346	0.577		-0.124	-0.255	0.227	
OV_N	0.201	0.172	-0.092	-0.493	-0.433		0.033		
SOL_AWC					-0.247				
ESCO		-0.384			-0.572	-0.651			
SOL_BD				-0.336	-0.219		0.058		

HCP with r > 0.5 are in bold.

Table 8. Range and average (in parentheses) of HSP from individual year (1992 to 2015) runs.

Parameter	ВС	BV	СН	LA
CN2	67.1 to 83.9 (76.7)	77.9 to 89.7 (84.5)	75.4 to 85.6 (81.5)	69.0 to 83.2 (75.8)
ALPHA_BF	0.035 to 0.127 (0.092)			
CH_N2	0.016 to 0.060 (0.033)		0.044 to 0.206 (0.104)	0.065 to 0.180 (0.112)
CH_K2		1.5 to 10.5 (7.7)	4.7 to 15.5 (10.1)	2.6 to 17.7 (9.6)
OV_N	0.022 to 0.591 (0.365)	0.101 to 0.441 (0.303)	0.206 to 0.572 (0.381)	0.274 to 0.585 (0.396)
ESCO		0.456 to 0.868 (0.612)		
SOL_BD				-0.431 to 0.443 (0.008)
Parameter	LN	MC	NI	WN
CN2	69.8 to 82.8 (77.8)	70.7 to 85.2 (77.7)		F(() 00 1 (01 F)
		70.7 10 65.2 (77.7)	47.9 to 76.3 (68.0)	76.6 to 90.1 (84.7)
CH_N2	0710 10 0_10 (1110)	70.7 to 65.2 (77.7)	47.9 to 76.3 (68.0) 0.018 to 0.283 (0.164)	76.6 to 90.1 (84.7)
CH_N2 CH_K2		4.0 to 23.1 (11.5)	` /	76.6 to 90.1 (84.7) 10.4 to 25.1 (16.8)
_	0.301 to 0.581 (0.410)	,	0.018 to 0.283 (0.164)	,
CH_K2	,	,	0.018 to 0.283 (0.164) 2.2 to 24.0 (13.4)	10.4 to 25.1 (16.8)
CH_K2 OV_N	0.301 to 0.581 (0.410)	,	0.018 to 0.283 (0.164) 2.2 to 24.0 (13.4)	10.4 to 25.1 (16.8)

Water 2020, 12, 2039 9 of 21

4.2.3. Final Calibration Year-By-Year Series

Information from the two prior modeling series was leveraged to improve calibration in the final year-by-year calibration series (2016 to 2018). Unacceptable objective metrics (RPS < 1.00 for Sens_Q) were used to omit the following basin–year combinations (BC-2016, BC-2018, NI-2017, and WN-2017).

Four model runs that were executed in this series, which include: (a) Global_Q that applied IT_Q parameter values (Tables 4 and 6) on a year-by-year basis (i.e., 2016 Global_Q); (b) Sens_Q in which variable, HSP (Table 8) were set between the range observed during the 1995 to 2015 runs; (c) SMERGE_Parameter (i.e., 2016 SMERGE_CN2); (d) PRISM_Parameter (i.e., 2016 PRISM_CN2). For the parameter-based model runs variable, HSP were set at ±10% of the average value obtained between 1995 to 2015 (Table 8), except for the highly correlated parameters (HCP). HCP values were calculated using the SMERGE 2.0 RZSM anomaly or raw PRISM precipitation for the examined year (i.e., 2016; Table 9) using the 1995 to 2015 regression relationship. The parameter range for HCP was set at ±10% of the calculated value.

4.3. Mass Balance Calculations

Streamflow (Q) simulated from year-by-year series (2016 to 2018) was compared against USGS gauge observed streamflow (with a nominal $\pm 10\%$ error). The range of simulated Q were produced by extracting all simulations in a model run that yielded acceptable results (RPS \geq 1.00). Streamflow was calculated based on mass balance within each basin based on:

$$Q_{Calculated} = P - \Delta S - ET$$
 (2)

where P was the annual average PRISM precipitation value within a watershed; ΔS was the change in annual terrestrial water determined from the GRACE product; ET was evapotranspiration and was estimated with three products (MODIS16A2v5; GLEAM v.3.3a; SSEBop v.4). A nominal 10% error was applied to calculated Q values. Note that LN-2018 was omitted in the mass balance analysis because of incomplete observed USGS streamflow data at the end of 2018.

5. Results

5.1. SWAT Simulations

The initial global series included Base_Q and IT_Q simulations. Only BV and CH have acceptable Base_Q simulations. The IT_Q results are dramatically better. Only MC was not satisfactory. BC, LA, NI, and WN were satisfactory to good, CH good to very good, and BV and NH exceeded the threshold for a very good simulation. Figure 3 combines the results from all eight basins into box plots. The average for the Base_Q model runs had an RPS value of 0.781, which was unacceptable. The iterative approach IT_Q improved objective results, with an average RPS of 1.886. T-test comparison between Base_Q and IT_Q simulations yielded a significant difference (based on t-test results) between the means of these model runs (p value = 0.0058). This comparison shows how constraining parameters improved model performance.

The final calibration year-by-year series had four types of model runs that included Global_Q, Sens_Q, SMERGE_Parameter, and PRISM_Parameter (Figure 4). Global_Q, which was based on IT_Q parameter values, had an average RPS of 1.282, considered satisfactory to good. In BC and NI, performance was unsatisfactory for all years (2016 to 2018). In other basins, simulations varied greatly on a year-by-year basis. In BV, results ranged from unsatisfactory to very good and in LA and MC, from unsatisfactory to good. LN recorded results between satisfactory and very good. In CH and WN, performance ranges between unsatisfactory to satisfactory.

The three other model series (Sens_Q, SMERGE_Parameter, and PRISM_Parameter) leveraged the results from the individual year-by-year simulation series (1995 to 2015) to constrain parameter values. These series yielded average RPS values (2.032 to 2.623), which ranged from good to very good in

Water 2020, 12, 2039 10 of 21

terms of performance. Notable improvements in the three-model series over Global_Q were noted for the following basin-year combination, which recorded an over 2.00 increase in RPS values (BV-2018, CH-2018, LA-2018, MC-2016, and NI-2016). Table 10 provided a summary of t-test results for these simulation series. The Global_Q model run had a statistically significant difference compared with the three other simulation series. Conversely, Sens_Q, SMERGE_Parameter, and PRISM_Parameter did not differ significantly between each other (Table 10). These results demonstrated a range of optimal solutions achieved with differing parameter values—a prime example of how equifinality can limit the utility of hydrologic simulations.

Table 9. Highly correlated parameter values for final calibration year-by-year (2016 to 2018) runs.

Basin	Year	Product	CN2	CH_K2	ESCO
BC	2017	SMERGE 2.0	78.5		
BC	2017	PRISM	82.5		
BV	2016	SMERGE 2.0	84.4	6.7	
BV	2016	PRISM	84.2	6.6	
BV	2017	SMERGE 2.0	81.0	4.1	
BV	2017	PRISM	80.2	3.5	
BV	2018	SMERGE 2.0	81.8	4.7	
BV	2018	PRISM	83.3	5.8	
CH	2016	SMERGE 2.0	81.2		
CH	2016	PRISM	81.6		
CH	2017	SMERGE 2.0	80.5		
CH	2017	PRISM	80.1		
CH	2018	SMERGE 2.0	80.1		
CH	2018	PRISM	83.7		
LA	2016	SMERGE 2.0		12.8	
LA	2016	PRISM		17.2	
LA	2017	SMERGE 2.0		7.1	
LA	2017	PRISM		7.6	
LA	2018	SMERGE 2.0		8.0	
LA	2018	PRISM		15.7	
LN	2016	SMERGE 2.0			0.824
LN	2016	PRISM			0.798
LN	2017	SMERGE 2.0			0.726
LN	2017	PRISM			0.761
LN	2018	SMERGE 2.0			0.798
LN	2018	PRISM			0.810
MC	2016	SMERGE 2.0	79.5		0.693
MC	2016	PRISM	85.1		0.943
MC	2017	SMERGE 2.0	77.5		0.602
MC	2017	PRISM	84.3		0.907
MC	2018	SMERGE 2.0	74.1		0.453
MC	2018	PRISM	81.1		0.764
NI	2016	SMERGE 2.0	62.4		
NI	2016	PRISM	67.1		
NI	2018	SMERGE 2.0	65.0		
NI	2018	PRISM	78.9		
WN	2016	SMERGE 2.0	85.0		
WN	2016	PRISM	89.2		
WN	2017	SMERGE 2.0	81.3		
WN	2017	PRISM	82.1		
WN	2018	SMERGE 2.0	80.3		
WN	2018	PRISM	85.5		

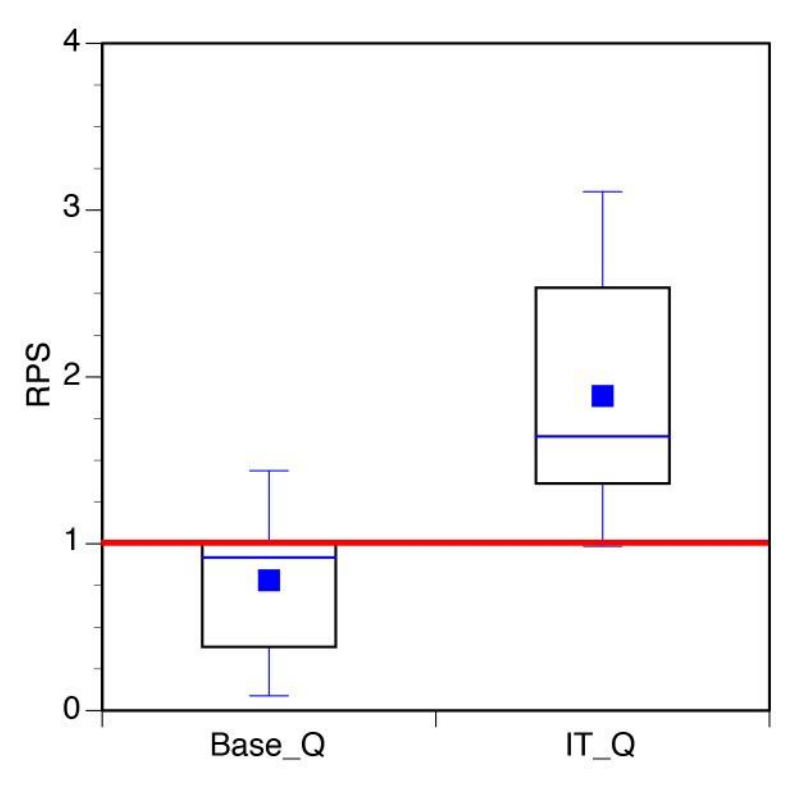


Figure 3. Combined RPS value from global simulation series (1995 to 2015). Red line represents an RPS **Figure 3.** Combined RPS value from global simulation series (1995 to 2015). Red line represents an **Example 2.00**, which is the threshold for an acceptable simulation. RPS = 1.00, which is the threshold for an acceptable simulation. **Table 10.** T-test comparison of mean RPS values from final year-by-year (2016 to 2018) runs.

	Model Run #1	on of mean RPS values from Model Run #2	m final yea p Value	r-by-year (2016 to 2018) runs. Degree of Significance
-	ModebaRun #1	Model_Run #2	Powalue	DegreegofySignificance
	Global O Global O Global O	SMERGE Parameter Sens O PRISM Parameter	0.0001 0.0309 0.0301	Highly Significant Highly Significant Significant Highly Significant
	Globa GobaQQ	SMERGE PRAMETER PRIBMI PROMETER	0.9 <u>9</u> 84 0.065 9	Highly Significant Significalistant
_	SMERGE Parameter	SMERGE arameter	0:5259	NNOS ignificant
50.16	Sens_Q	PRISM_Parameter	0.0659	Not Significant
5.2. Mass	Balance Comparisons SMERGE_Parameter	PRISM_Parameter	0.1452	Not Significant

To avoid the equifinality constraint, calculated Q, which used P, ET, and ΔS , was examined. This Have Compared in Figures 5-10 for the years 2016 to 2018 TSimilar results were obtained in most the watersheds as discussed below. Note that BC-2016, was examined. BG52P18a, 95WNI-29177. Water, mitted begatter go acceptable simulations were obtained yearing others 2018. Similar results were obtained in most the watersheds, as discussed below. Note that BC-2016, BC-2678, White A12697 Weter on mice wets compared poorly against USGS, gauge to be even and in general As 20 feb. was restimated this value pMODIS16 A2 v5. nearly always sens rated a chiebly sinflated calculated. At a layer of Lift Mr. v3. 3 a and cs. EBMP x-6 exhibited agains y u is bill leave the general tendency to stroduce an overestimate rule: Notate 16 A 2 CF FEAM, valvay By EART and A AND IN MATERIAL and Mac-2017 a Figures EAMV and and south SSEP park to letter 18016 va A a 2011 von the NI 18017 in Figure far Figure 7b to 30 Figure 1 Overederiestimated cubserved. Que Navostburgo timos 7, espectivel M Quitof the 20 exertable hasing of the North sear can bise tions of the North and the North an MOPUSI 6A3275 SMC 5201 613894 MC 27017; Figure 84th en, despectively don SI the 2N 2023 30 abilities in the contraction of the GH-2017, MCt-2016; and MC-2017; Figures 5a of hand fail he declarated with the nominal observed to bandussebor, racalculated Ramatched slightly better with the Borzion, correspondently in the sixth sixth 2017, And years combinations (ARC-2017 with the 170 Interest to be 1807-2016, 1807-2016, 1807-2016) and CHEN 3017 his setter while the honfiled to be regarded by the light beginning the combinations

(BC-2017, CH-2017, LA-2016, LN-2016, MC-2016, MC-2017, WN-2016, and WN-2017; Figures 5a, 6b,

7a, 8 Samparing Let products, generally, MODIS16A2v5 yielded the highest calculated Q and SSEBop v.4 the owners of calculated products, generally, MODIS16A2v5 yielded the highest calculated Q and SSEBop v.4 the owners of calculated products, generally, MODIS16A2v5 yielded the highest calculated Q and SSEBop v.4 the owners of calculated products, generally, MODIS16A2v5 yielded the highest calculated Q and SSEBop v.4 the owners of calculated Q value. For MC-2016 (Figure 9a), SSEBop v.4 had the highest

valuenterms of the final calibration year-by-year series, the simulated Q much better matched with Interest the final calibration year-by-year series, the simulated Q much better matched with Interest the final calibration years by year series, the simulated Q much better matched with Interest the final calibration years by year series, the simulated Q much better matched with Interest the simulated Angeles and the series of the series of

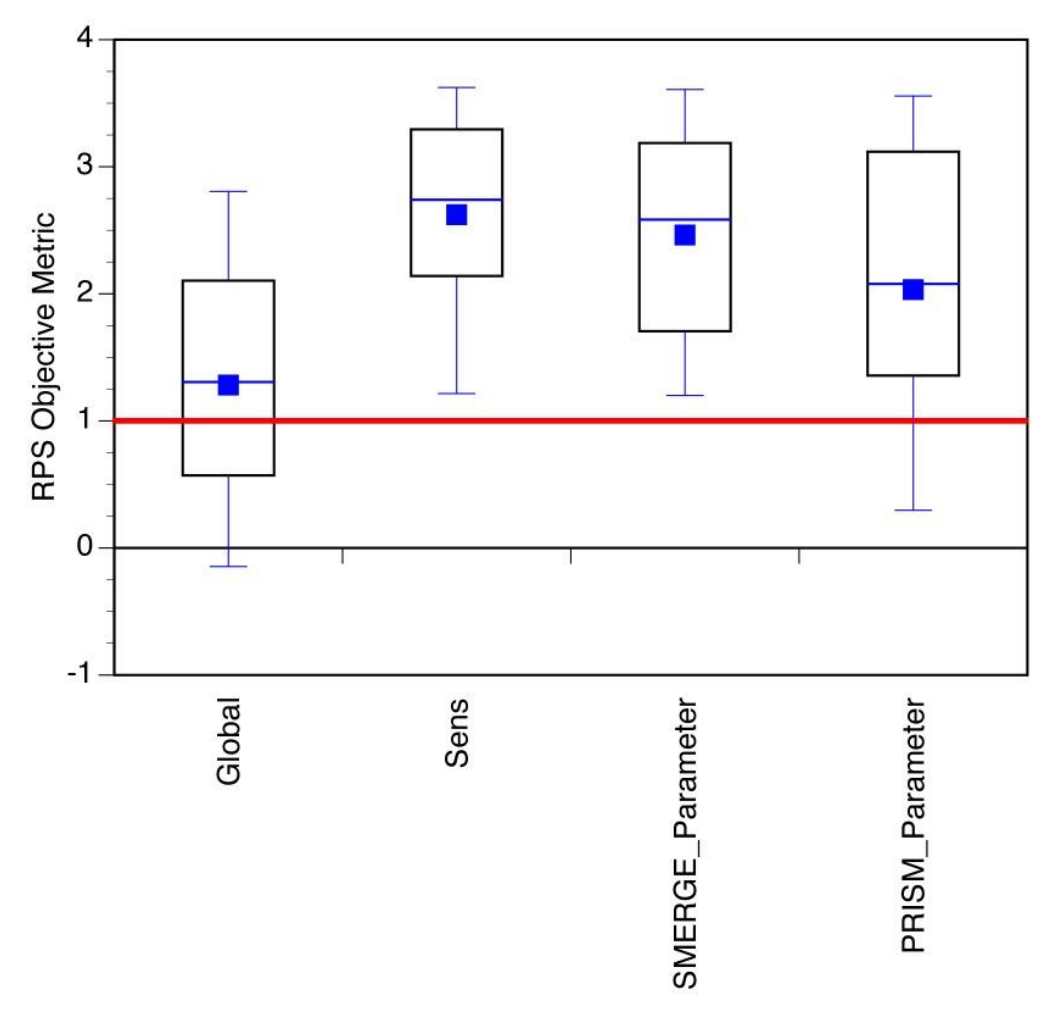


Figure 4. Combined RPS value from final year-by-year series (2016 to 2018). Red line represents an RPS = 1.00, which is the threshold for an acceptable simulation.

Water 2020, 12, 2039 13 of 21

6. Discussion

Water **2020**, 12, x FOR PEER REVIEW

14 of 22

This work is a fundamental example of how constraining parameter values in a hydrologic model can improve USSicologic performance measures during autocalibration. Even so the issue of equifinality remains (e.gh.§3%) rk During damodal example of wore colored in my place of equifinality remains (e.gh.§3%) rk During damodal example of wore colored in my place of equifinality implementations at hydrologic toologic toologic toologic principles of the colored in my place of the col

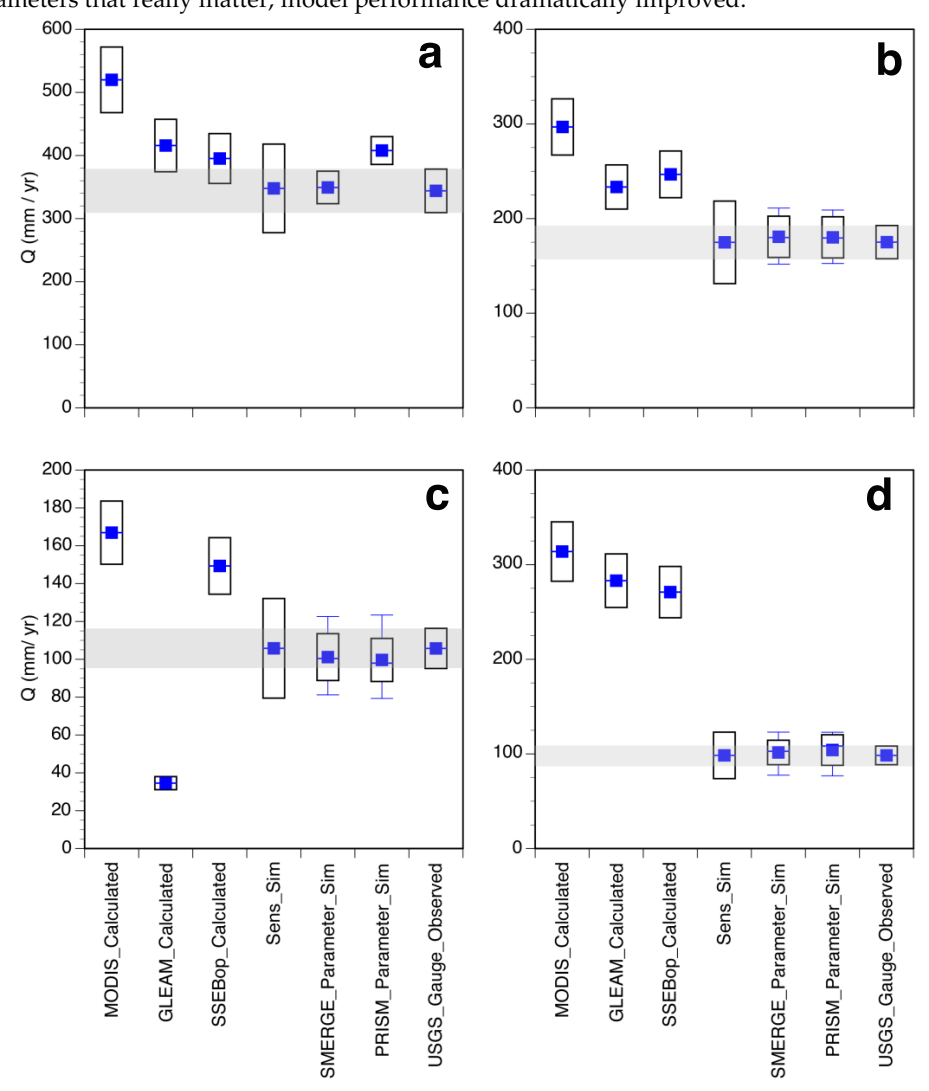


Figure 5. Observed USGS, mass balance calculated with the Moderate Resolution Imagining Spectrometer, MODIS16A2v5 (MODIS), balance calculated with the Moderate Resolution Imagining Spectrometer, MODIS16A2v5 (MODIS), Global Land Evaporation: the Amsterdam Model (GLEAM), Simplified Surface Energy Balance (SSEBop), and final calibration year-by-year SWA1 simulated Simplified Surface Energy Balance (SSEBop), and final calibration year-by-year SWA1 simulated Simplified Surface Energy Balance (SSEBop), and final calibration year-by-year SWA1 simulated (Sens_Q SMERGE_Parameter_PRISM_Parameter) streamflow (Q). Gray field indicates nominal ±10% error of USGS streamflow observations (a) BC 22016 (b) BV-2016 (c) BV-2017, and (d) BV-2018.

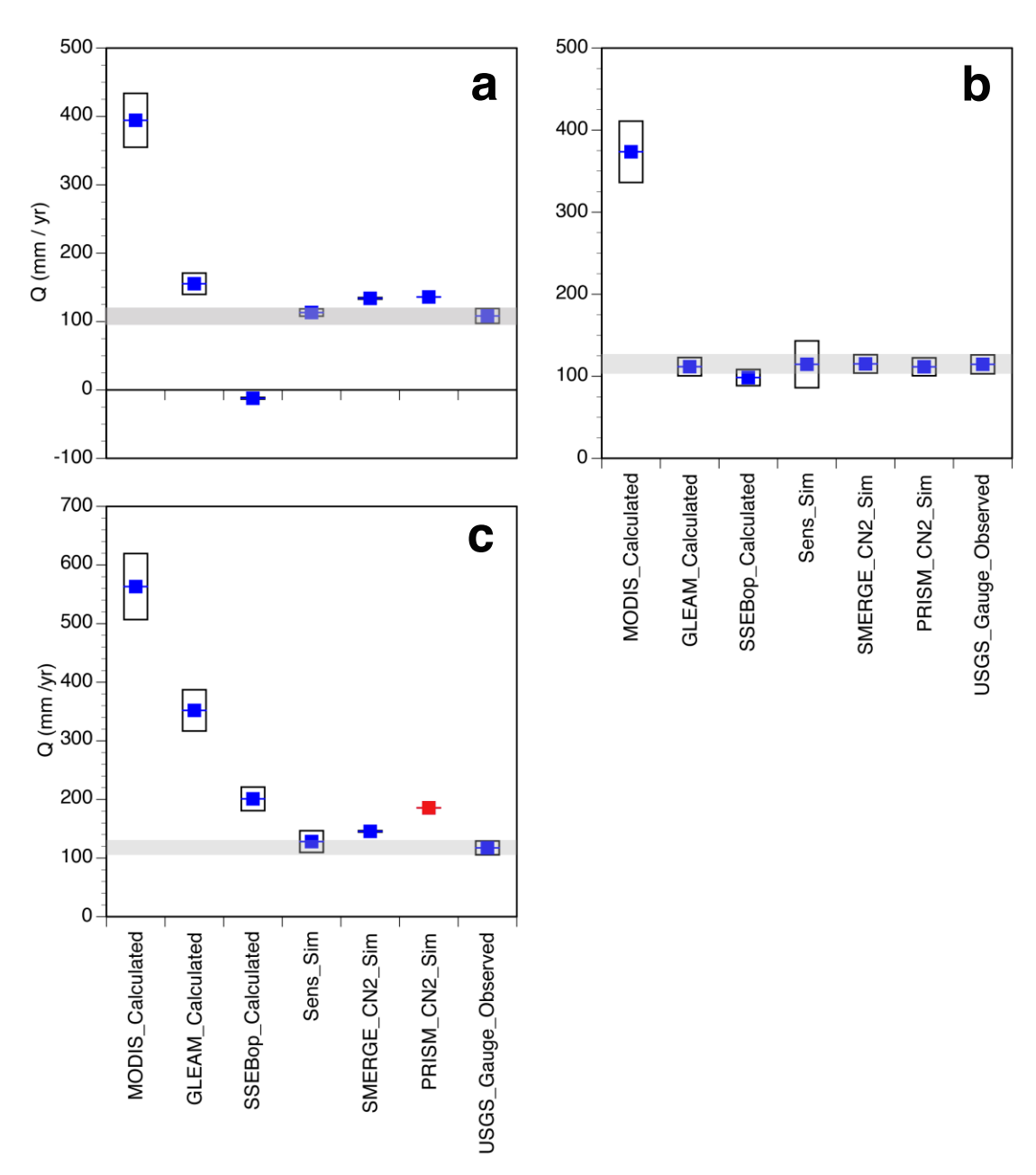


Figure 6. Same as Figure 5, except red symbol indicates an unacceptable simulation (RPS < 1.00). (a) The form of the content o

Another interesting result was the slight preference for leveraging RZSM (SMERGE 2.0) over precipitation (RRISMingresophwaisthmodelphyprofenamee for This reginty RIZSMI (SMERGE 2.0) over precipitation (RRISMingresophwaisthmodelphyprofenamee for This reginty RIZSMI (SMERGE 2.0) over precipitation (RRISMingresophwaisthmodelphyprofenamee for This reginty RIZSMI (SMERGE 2.0) over precipitation (RRISMingresophwaisthmodelphyprofenamee for This reginty RIZSMI (SMERGE 2.0) over precipitation (RRISMI) interesting the statistic of the precipitation of the subject o

Metter Particelle of SWAT has issues with the direct assimilation of soil moisture data [24]. EPf stanother important flux with the water budget at a watershed scale. In the mass balance approach, utilized ET is at least two orders of magnitude greater than AS. The fact that PRISM precipitation data another important flux with the water budget at a watershed scale. In the mass balance approach, was used to drive SWAT simulations and that robust results were obtained supports the general utilized ET is at least two orders of magnitude greater than AS. The fact that PRISM precipitation accuracy of this dataset. Therefore, the discrepancies that exist between the calculated and simulated accuracy of this dataset. Therefore, the discrepancies that exist between the calculated and simulated Q values must largely lay with three ET datasets used in this study. MODISA 25 tends to perform accuracy of this datasets. Therefore, the discrepancies that exist between the calculated and simulated less well in the central Great Plains, where there is a more limited vegetation cover [42]. The GLEAM Q values must largely lay with three ET datasets used in this study. MODISA 25 tends to perform product also had issues in this region. At its core, GLEAM assimilates satellite estimated precipitation less well in the central Great Plains, where there is a more limited vegetation cover [42]. The GLEAM that has a strong tendency to overestimate summertime particularly over the Great Plains [43,44]. These errors can generate a strong positive bias in annual ET estimates from this region. Because of these errors can generate a strong positive bias in annual ET estimates from this region. Because of these issues, we opted not to utilize data from these ET products to constrain SWAT parameter. These errors can generate a strong positive bias in annual ET estimates from this region. Because of these issues, we opted not to utilize data from these ET products to constrain SWAT parameter.

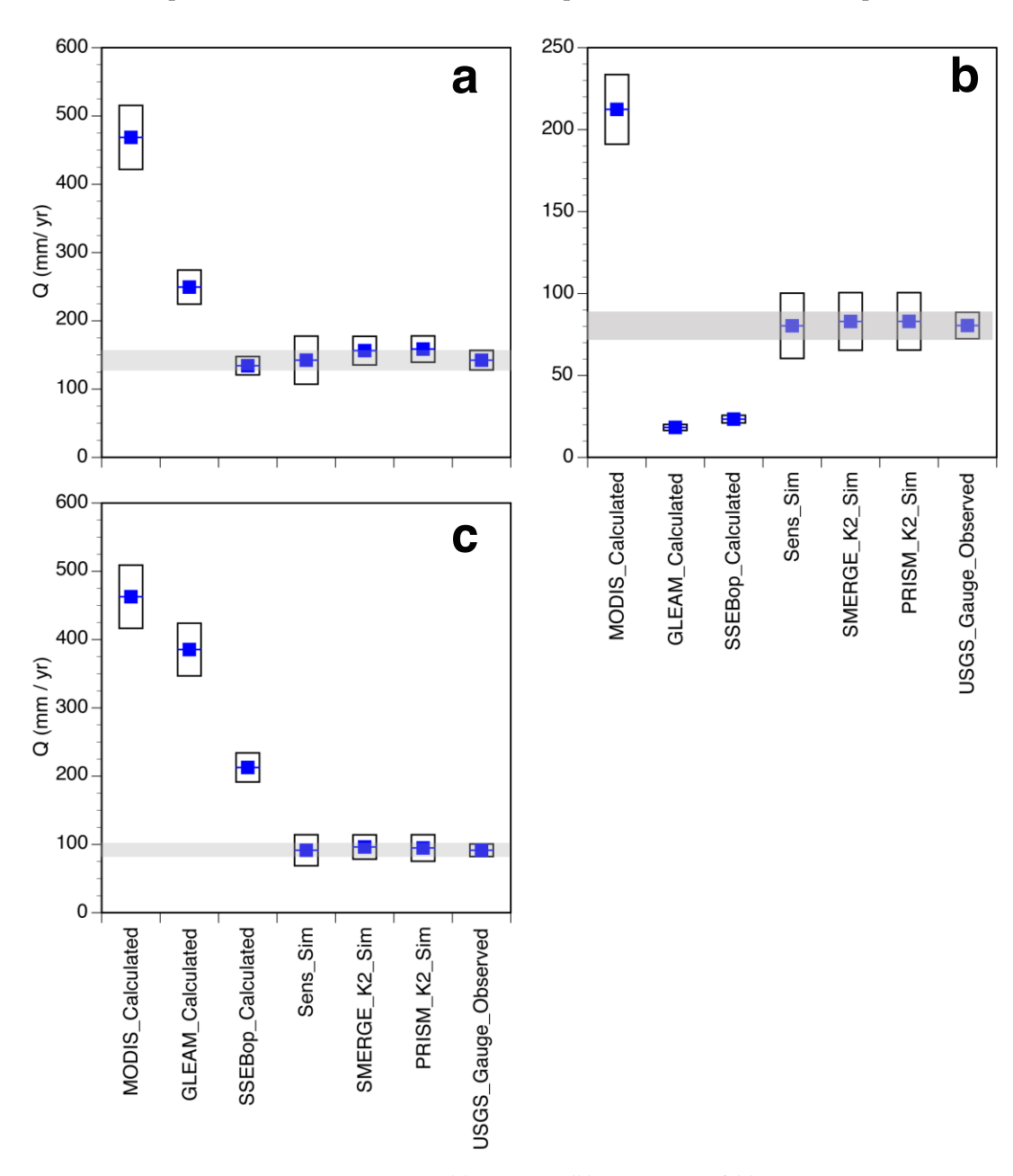


Figure 7. Same as Figure 5. (a) LA-2016, (b) LA-2017, and (c) LA-2018.

Figure 7. Same as Figure 5. (a) LA-2016, (b) LA-2017, and (c) LA-2018.

Water 2020, 12, x FOR PEER REVIEW

17 of 22

Future work will further validate the approaches articulated in this study beyond the Great Plains within a broadwangeok wild twiters, velidated throughout office this study strange the Great provided in the stark and from the stark and the stark and of the ation of the atio Califorallapson destructional estimates to Califoralla Sauthenne Authorn the Consust Plains, the General Valley regions, finalitoring a march word in both Southwestern with heartern GON URe In bighty aforested provides ionseinduding our zon. In the wastern and Faster's Gandelis Candelis Likel North may corn battexidendilegttemestimate of IRZSIM SIMERICLETED at societaen Senthann and itential terational and the estima cerrof rezisant and interferente lawa testilippisus SMFEGEn 2 Winter colorise from the land houristage model estimates imates refir ZSM arther taker able ale tenesten plynier pod estimates imates allithricismoisture moisturetimates apreficited britands of rezemodel or merged land surface model and the satellite soil moisture retrievals yield optimal estimates of RZSM [22].

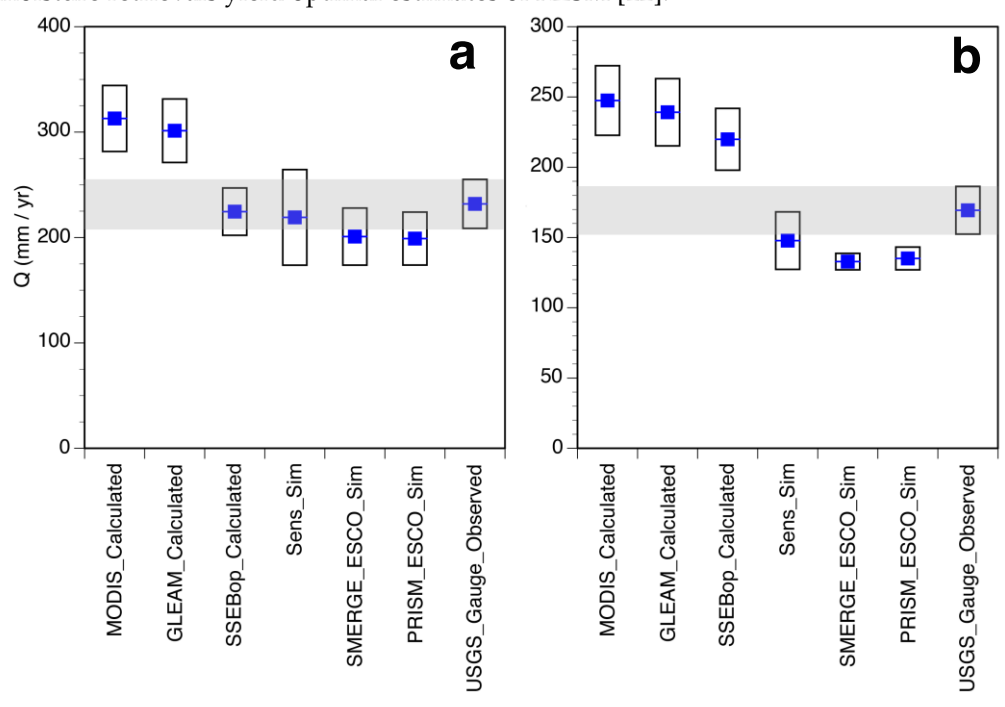


Figure & Sames Figures Figure 9. 791 (N-2016) Lind 701 ZN-2017.

7. Conclusions 7. Conclusions

To summarize, the key results are as follows:

To summarize, the key results are as follows:

(1) The final calibration year-by-year simulation series (2016 to 2018), which was based on executing SWAT on an annual basis, outperformed the global simulations series, in which one objective (1) The final calibration year-by-year simulation series (2016 to 2018), which was based on metric was calculated based on the entire analysis period (1995 to 2015) and the entire analysis period (1995 to 2015). Which was based on executing SWAT on an annual basis, outperformed the global simulations series, in which one (2) For the final calibration year-by-year simulation series, four model runs was calculated based on the entire analysis period (1995 to 2018), which was calculated based on the entire analysis period (1995 to 2018).

(Global Q; Sons Q; SMERGE Parameter; PRISM Parameter) The Global Q simulation which was ecuted based on parameter values hixed during the global simulation series hunderper formed compared was with other model runs in which parameter values were sonstrained with information derived from dwith individual year-by-year models as well as SMERGE 20 RZSM anomaly and PRISM precipitation data from

(3) nSMERGE-Parameter simulations we had slightly highers RPS notable and present precipitation PRISM_dParameter simulations and also better matched with USGS gauge observed Q.

(4) Calculated Resection a mass balance approach did not consistently match observed Quiplike with SWAT simulated Q. The highest calculated Q was vielded by using the MQDIS16A2v5 ET product, followed by GIEAMING 3a and SSEBop v.4 which best matched with observed Q unlike SWAT simulated Q. The highest calculated Q was yielded by using the MODIS16A2v5 ET product, followed by GLEAM v.3.3a, and SSEBop v.4, which best matched with observed Q.

The significant implication derived from this work is the demonstration that constraining parameter values can markedly improve SWAT model performance. In addition, that RZSM from SMERGE 2.0 can be leveraged to also greatly improve SWAT model performance. Therefore, this Water **2020**, 12, 2039

The significant implication derived from this work is the demonstration that constraining parameter values can markedly improve SWAT model performance. In addition, that RZSM from 18 of 22 SMERGE 2.0 can be leveraged to also greatly improve SWAT model performance. Therefore, this work work highlights how diverse remote sensing data can be used to support hydrologic modeling of streamflow streamflow at the watershed scale providing more physically realistic results.

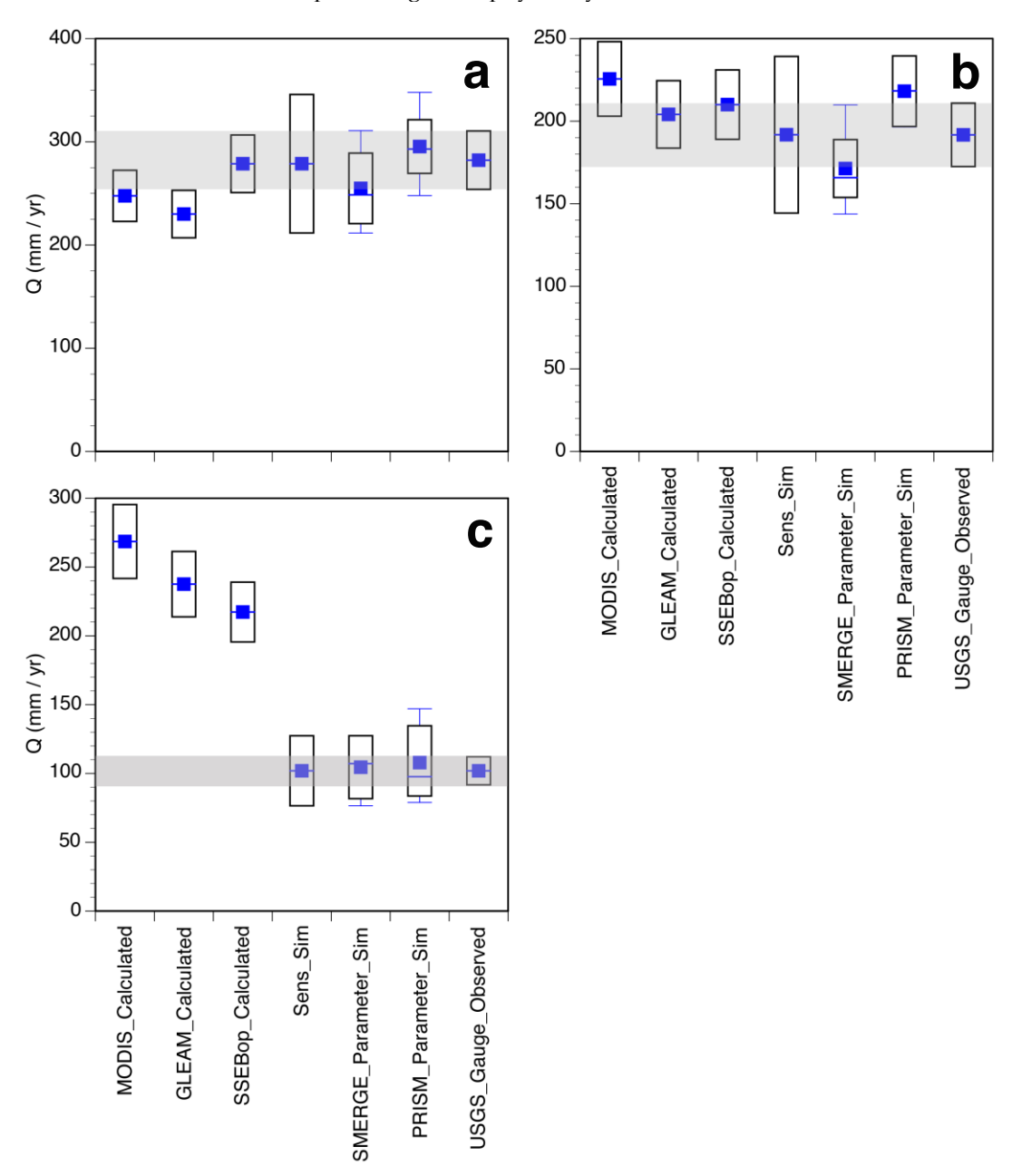


Figure 9. Same as Figure 5. (a) MC-2016, (b) MC-2017, and (c) MC-2018. **Figure 9.** Same as Figure 5. (a) MC-2016, (b) MC-2017, and (c) MC-2018.

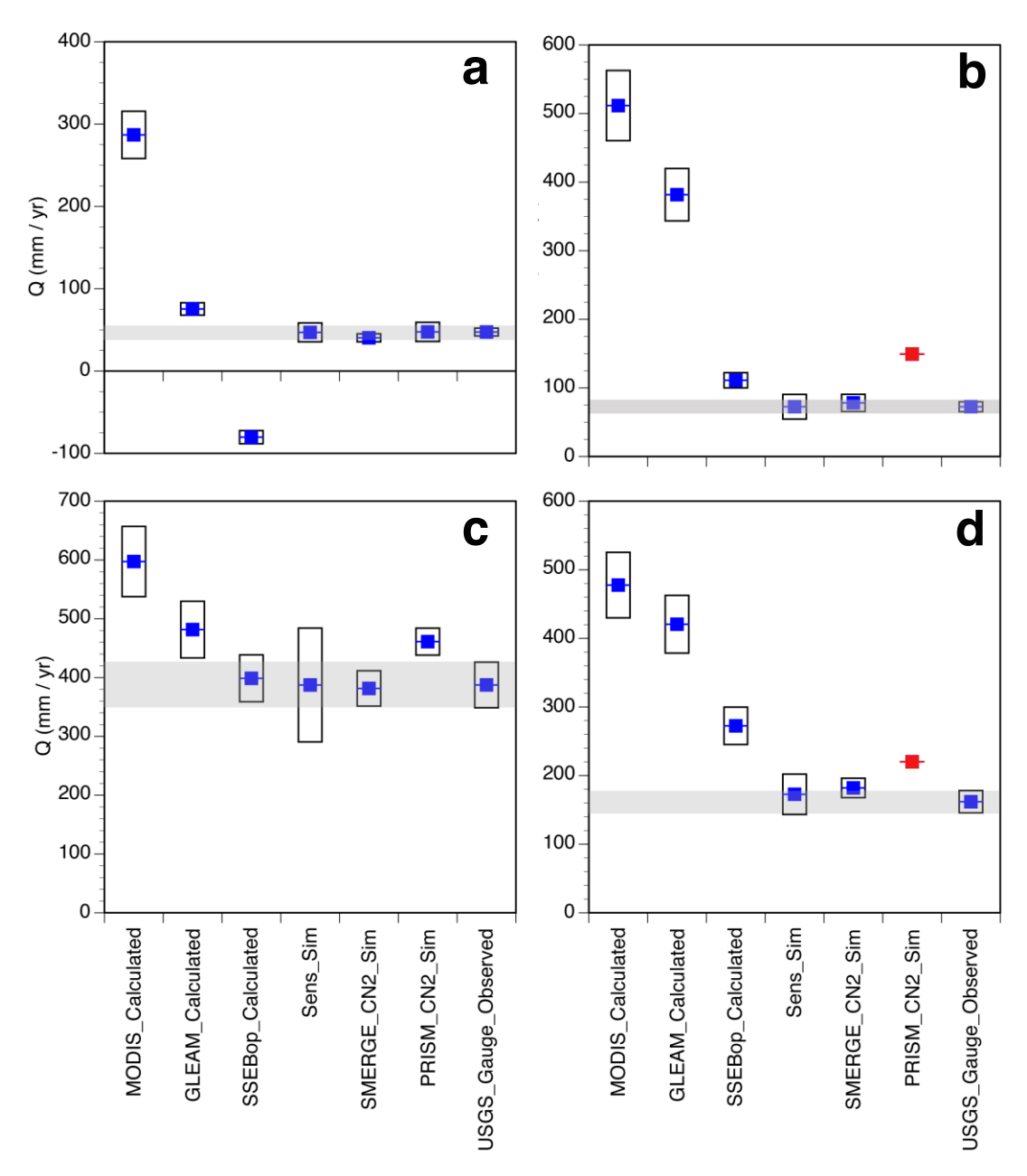


Figure 10. Same as Figure 5, except red symbol indicates an unacceptable simulation (RPS < 1.00). (a) NI-2016, (b) NI-2018, (c) WN-2016, and (d) WN-2018. **Figure 10.** Same as Figure 5, except red symbol indicates an unacceptable simulation (RPS < 1.00). (a) NI-2016, (b) NI-2018, (c) WN-2016, and (d) WN-2018.

Author Contributions: Conceptualization, K.J.T.; methodology, K.J.T.; validation, K.J.T.; formal analysis, Author Contributions. Conceptualization, K.J.T.; detectedations, K.J.T.; waiting ion regime from parameters. J.T.; funding acquisition, K.J.T.; M.E. Burrisualization, K.J.T.; funding acquisition, K.J.T. All authors have read and agreed to the published version of the manuscript. R.J.T.; funding acquisition, K.J.T.; M.E.B.; visualization, K.J.T.; Supervision, K.J.T.; project administration, K.J.T.; funding. N.A.A. (Internal dispersed and edition). R.J.T.; M.E.B.; visualization, K.J.T.; M.E.B.; visualization, M.E.B.; visualization, K.J.T.; M.E.B.; visualization, M.E.B.; vis

fur Funding UNANA (Runte And dicators and Water Broducts for Future National Climate Assessments program through award # NNX16AH30G and NSF Geoscience Equipment (Award Number 1636769).

Funding: NASA Climate Indicator and Data Products for Future National Climate Assessments program

Funding: NASA Climate Indicator and Data Products for Future National Climate Assessments program
Acknowledgments: The assistance of Arturo Diaz (Texas A&M International University) is greatly appreciated.
through award # NNX16AH30G and NSF Geoscience Equipment (Award Number 1636/69).

Conflicts of Interest: The authors declare no conflict of interest. The funders had no role in the design of the Acknowledge of the Acknowledge of the Acknowledge of Acknowledge of the Acknowledge of the

study; in the collection, analyses, or interpretation of data; in the writing of the manuscript, or in the decision to

publish the results.

Water 2020, 12, 2039 19 of 21

References

1. Gassman, P.W.; Reyes, M.R.; Green, C.H.; Arnold, J.G. The Soil and Water Assessment Tool: Historical development, applications, and future research directions. *Trans. ASABE* **2007**, *50*, 1211–1250. [CrossRef]

- Zeiger, S.J.; Hubbart, J.A. A SWAT model validation of nested-scale contemporaneous streamflow, suspended sediment and nutrients from a multiple-land-use watershed of the central USA. Sci. Total Environ. 2016, 572, 232–243. [CrossRef] [PubMed]
- 3. Akay, H.; Kocyigit, M.B.; Yanmaz, A.M. Effect of using multiple stream gauging stations on calibration of hydrologic parameters and estimation of hydrograph of ungauged neighboring basin. *Arab. J. Geosci.* **2018**, 11, 282. [CrossRef]
- 4. Xie, H.; Longuevergne, L.; Ringler, C.; Scalon, B.R. Calibration and evaluation of a semi-distributed watershed model of Sub-Saharan Africa using GRACE data. *Hydrol. Earth Syst. Sci.* **2012**, *9*, 3083–3099. [CrossRef]
- 5. Qiao, L.; Herrmann, R.B.; Pan, Z. Parameter uncertainty reduction for SWAT using GRACE, streamflow, and groundwater table data for the Lower Missouri River Basin. *J. Am. Water Resour. Assoc.* **2013**, 49, 343–358. [CrossRef]
- 6. Kundu, D.; Vervoort, R.W.; van Ogtrop, F.F. The value of remotely sensed surface soil moisture for model calibration using SWAT. *Hydrol. Process.* **2017**, *31*, 2764–2780. [CrossRef]
- 7. Nilawar, A.P.; Calderella, C.P.; Lakhankar, T.Y.; Waikar, M.L. Satellite soil moisture validation using hydrological SWAT Model: A case study of Puerto Rico, USA. *Hydrology* **2017**, *4*, 45. [CrossRef]
- 8. Azimi, S.; Dariane, A.B.; Modanesi, S.; Bauer-Marschallinger, B.; Bindlish, R.; Wagner, W.; Massari, C. Assimilation of Sentinel 1 and SMAP—Based satellite soil moisture retrievals into SWAT hydrological model: The impact of satellite revisit time and product spatial resolution on flood simulations in small basins. *J. Hydrol.* 2020, 581, 124367. [CrossRef]
- 9. Abiodun, O.O.; Guan, H.; Post, V.E.A.; Batelaan, O. Comparison of MODIS and SWAT evapotranspiration over a complex terrain at different spatial scales. *Hydrol. Earth Syst. Sci.* **2018**, 22, 2775–2794. [CrossRef]
- 10. Rajib, A.; Merwade, V.; Yu, Z. Rationale and efficacy of assimilating remotely sensed potential evapotranspiration for reduced uncertainty of hydrologic models. *Water Resour. Res.* **2018**, *54*, 4615–4637. [CrossRef]
- 11. Tobin, K.J.; Bennett, M.E. Improving alpine summertime streamflow simulations by incorporation of evapotranspiration data. *Water* **2019**, *11*, 112. [CrossRef]
- Fallatah, O.A.; Ahmed, M.; Cardace, D.; Boving, T.; Akanda, A.S. Assessment of modern recharge to arid region aquifers using an integrated geophysical, geochemical, and remote sensing approach. *J. Hydrol.* 2019, 569, 600–611. [CrossRef]
- 13. Milewski, A.; Seyoum, W.M.; Elkadiri, R.; Durham, M. Multi-scale hydrologic sensitivity to climatic and anthropogenic changes in Northern Morocco. *Geosciences* **2020**, *10*, 13. [CrossRef]
- 14. Xie, X.; Zhang, D. Data assimilation for distributed hydrological catchment modeling via ensemble Kalman filter. *Remote Sens. Environ.* **2010**, 33, 678–690. [CrossRef]
- 15. Liu, Y.; Wang, W.; Liu, Y. ESA CCI Soil moisture assimilation in SWAT for improved hydrological simulation in Upper Huai River Basin. *Adv. Meteorol.* **2018**, 7301314. [CrossRef]
- 16. Patil, A.; Ramsankaran, R. Improved streamflow simulations by coupling soil moisture analytical relationship in EnKF based hydrological data assimilation framework. *Adv. Water Resour.* **2018**, *121*, 173–188. [CrossRef]
- 17. Chen, F.; Crow, W.T.; Starks, P.J.; Moriasi, D.N. Improving hydrologic predictions of a catchment model via assimilation of surface soil moisture. *Adv. Water Resour.* **2011**, *34*, 526–536. [CrossRef]
- 18. Arnold, J.G.; Allen, P.M. Estimating hydrologic budgets for three Illinois watersheds. *J. Hydrol.* **1996**, 176, 57–77. [CrossRef]
- 19. Xu, C.Y. Climate change and hydrologic models: A review of existing gaps and recent research developments. *Water Resour. Manag.* **1999**, *13*, 369–382. [CrossRef]
- 20. Berger, K.P.; Entekhabi, D. Basin hydrologic response relations to distributed physiographic descriptors and climate. *J. Hydrol.* **2001**, 247, 169–182. [CrossRef]
- 21. Lettenmaier, D.P. Observations of the Global Water Cycle—Global Monitoring Networks. In *Encyclopedia of Hydrologic Sciences*; Anderson, M.G., McDonnell, J.J., Eds.; J. Wiley and Sons Publishers: Hoboken, NJ, USA, 2005; Volume 5, pp. 2719–2732.

Water 2020, 12, 2039 20 of 21

22. Tobin, K.J.; Crow, W.T.; Dong, J.; Bennett, M.E. Validation of a new soil moisture product Soil MERGE or SMERGE. *IEEE J. Sel. Top. Appl. Earth Obs. Remote Sens.* **2019**, *12*, 3351–3365. [CrossRef]

- Running, S.; Mu, Q.; Zhao, M. MOD16A2 MODIS/Terra Net Evapotranspiration 8-Day L4 Global 500m SIN Grid V006 [Data set]; NASA EOSDIS Land Processes DAAC. 2017. Available online: https://doi.org/10.5067/ MODIS/MOD16A2.006 (accessed on 21 April 2020).
- 24. Senay, G.B.; Budde, M.; Verdin, J.P.; Melesse, A.M. A coupled remote sensing and simplified surface energy balance approach to estimate actual evapotranspiration from irrigated fields. *Sensors* **2007**, *7*, 979–1000. [CrossRef]
- 25. Martens, B.; Miralles, D.G.; Lievens, H.; van der Schalie, R.; de Jeu, R.A.M.; Fernández-Prieto, D.; Beck, H.E.; Dorigo, W.A.; Verhoest, N.E.C. GLEAM v3: Satellite-based land evaporation and root-zone soil moisture. *Geosci. Model Dev.* 2017, 10, 1903–1925. [CrossRef]
- 26. Watkins, M.M.; Wiese, D.N.; Yuan, D.-N.; Boening, C.; Landerer, F.W. Improved methods for observing Earth's time variable mass distribution with GRACE using spherical cap mascons. *J. Geophys. Res. Solid Earth* **2015**, *120*, 2648–2671. [CrossRef]
- 27. Wiese, D.N.; Landerer, F.W.; Watkins, M.M. Quantifying and reducing leakage errors in the JPL RL05M GRACE mascon solution. *Water Resour. Res.* **2016**, *52*, 7490–7502. [CrossRef]
- 28. Myneni, R.; Knyazikhin, Y.; Park, T. MOD15A2H MODIS/Terra Leaf Area Index/FPAR 8-Day L4 Global 500m SIN Grid V006 [Data set]; NASA EOSDIS Land Processes DAAC. 2015. Available online: https://doi.org/10.5067/MODIS/MOD15A2H.006 (accessed on 21 April 2020).
- 29. Neitsch, S.L.; Arnold, J.G.; Kiniry, J.R.; Srinivasan, R.; Williams, J.R. *Soil and Water Assessment Tool User's Manual*; Texas Water Resource Institute Report TR-192; Texas Water Resource Institute: College Station, TX, USA, 2002; Available online: https://swat.tamu.edu/media/1294/swatuserman.pdf (accessed on 1 March 2020).
- 30. Williams, J.R. Flood routing with variable travel time or variable storage coefficients. *Trans. ASABE* **1969**, 12, 100–103. [CrossRef]
- 31. Abbaspour, K.C.; Yang, J.; Maximov, L.; Siber, R.; Bogner, K. Modeling hydrology and water quality in the pre-alpine/alpine Thur watershed using SWAT. *J. Hydrol.* **2007**, 333, 413–430. [CrossRef]
- 32. Yang, J.; Reichert, P.; Abbaspour, K.C.; Xia, J.; Yang, H. Comparing uncertainty analysis techniques for SWAT application to the Chaoche Basin in China. *J. Hydrol.* **2008**, *358*, 1–23. [CrossRef]
- 33. Uniyal, B.; Jha, M.K.; Verma, A.K. Parameter identification and uncertainty analysis for simulating streamflow in a river basin of Eastern India. *Hydrol. Process.* **2015**, *29*, 3744–3766. [CrossRef]
- 34. Tobin, K.J.; Bennett, M.E. Satellite precipitation products and hydrologic applications. *Water Int.* **2014**, *39*, 360–380. [CrossRef]
- 35. Moriasi, D.N.; Arnold, J.G.; Van Liew, M.W.; Bingner, R.L.; Harmel, R.D.; Veith, T.L. Model evaluation guidelines for systematic quantification of accuracy in watershed simulations. *Trans. ASABE* **2007**, *50*, 885–900. [CrossRef]
- 36. Galdos, F.V.; Alvarex, C.; Garcia, A.; Revilla, J.A. Estimated distributed rainfall interception using a simple conceptual model and Moderate Resolution Imaging Spectroradiometer (MODIS). *J. Hydrol.* **2012**, 468, 213–228. [CrossRef]
- 37. Arnold, J.G.; Allen, P.M. Automated methods for estimating baseflow and groundwater recharge from stream flow records. *J. Am. Water Resour. Assoc.* **1999**, 35, 411–424. [CrossRef]
- 38. Beven, K.; Freer, J. Equifinality, data assimilation, and uncertainty estimation in mechanistic modeling of complex environmental systems using the GLUE methodology. *J. Hydrol.* **2001**, 249, 11–29. [CrossRef]
- 39. Fu, C.; James, A.L.; Yao, H. Investigations of uncertainty in SWAT hydrologic simulations: A case study of a Canadian Shield catchment. *Hydrol. Process.* **2015**, *29*, 4000–4017. [CrossRef]
- 40. Her, Y.; Chaubey, I. Impact of the numbers of observations and calibration parameters on equifinality, model performance, and output and parameter uncertainity. *Hydrol. Process.* **2015**, 29, 4220–4237. [CrossRef]
- 41. Rajib, M.A.; Merwade, V. Improving soil moisture accounting and streamflow prediction in SWAT by incorporating a modified time-dependent Curve Number method. *Hydrol. Process.* **2016**, *30*, 603–624.
- 42. Velpuri, N.M.; Senay, G.B.; Singh, R.K.; Bohms, S.; Verdin, J.P. A comprehensive evaluation of two MODIS evapotranspiration products over the conterminous United States: Using point and gridded FLUXNET and water balance ET. *Remote Sens. Environ.* **2013**, *139*, 35–49. [CrossRef]

Water **2020**, 12, 2039

43. Ebert, E.E.; Janowiski, J.E.; Kidd, C. Comparison of near-real-time precipitation estimates from satellite observations. *Bull. Am. Meteorol. Soc.* **2007**, *88*, 47–64. [CrossRef]

44. Tian, Y.; Peters-Lidard, C.D.; Choudhury, B.J.; Garcia, M. Multi-temporal analysis of TRMM-based satellite precipitation products for land data assimilation applications. *J. Hydrometeorol.* **2007**, *8*, 1165–1183. [CrossRef]



© 2020 by the authors. Licensee MDPI, Basel, Switzerland. This article is an open access article distributed under the terms and conditions of the Creative Commons Attribution (CC BY) license (http://creativecommons.org/licenses/by/4.0/).